International Journal of Modern Physics A
Vol. 35, No. 26 (2020) 2050161 (10 pages)

DOI: 10.1142/S0217751X20501614

World Scientific
www.worldscientific.com

Statefinder diagnostic for exponential harmonic field

A. D. Kanfon*

Faculté des Sciences et Techniques,
Université Nationale des Sciences, Technologies,
Ingénerie et Mathématiques, Abomey, Bénin
kanfon@yahoo.fr

F. Mavoa

Chaire internationale en Physique mathématique et Applications,
Université d'Abomey-Calavi, Bénin
maferdson@yahoo.fr

G. Koto N'Gobi

Faculté des Sciences et Techniques, Université d'Abomey-Calavi, Bénin
kotgabin36@yahoo.fr

Received 29 March 2020
Accepted 24 August 2020
Published 21 September 2020

The dynamic study of the harmonic exponential field has been made using the statefinder diagnostic. By the use of a specific method, we find out the statefinder parameters r, s according to the deceleration parameter and the redshift. The numerical analysis of these parameters brings out the transition between the accelerated and decelerated phases of the universe. There is also an attracting effect from the SCDM (Standard Cold Dark Matter) model toward the LCDM model (ΛCDM). In view of the results this study allows us to classify the exponential harmonic field among the quintessential models.

Keywords: Harmonic exponential field; statefinder parameters; statefinder diagnostic.

PACS numbers: 98.80.Bp, 98.80.Cq

1. Introduction

Observations have shown that our universe is in an accelerated expansion phase.[1–5] Among other observations, we can mention supernovae type Ia (SNIa),[6] CMB,[7] WMAP (Wilkinson Microwave Anisotropy Probe).[7]

*Corresponding author.

The enigmatic dark energy would be responsible for this behavior of the universe and is characterized by negative pressure.[1,2,8] The cosmological constant is the simplest dark energy model characterized by constant pressure over time.[8] However, taking into account such energy poses some problems. First, if this constant exists, it must be small in time, and it is precisely this smallness at the level of fundamental interactions that is difficult to admit especially in high energy physics. Second, why this form of energy has proved today the most important and therefore the most dominant of the universe? All these problems have led scientists to undertake researches implementing other models of dark energy. Recent observations of SNIa have shown that dark energy as a function of time gives a better fit than the cosmological constant.[6] This assumption of dark energy as a function of time makes it possible to study the dynamics of dark energy. For this approach, several models have been considered among which the most famous is the quintessence model.[9,10]

Other models of energy were considered for instance the ghost model;[11,12] the tachyonic model;[13] the quintome model;[14] the Chaplygin gas model,[15,16] etc. Since there is more and more models that can express the expansion of the universe, it would be desirable to find a way to be able to discriminate each competing model. And it is in this perspective that Sahni *et al.*[17] recently proposed a pair of cosmological diagnostics r, s called statefinder and is defined as follows:

$$r = \frac{\dddot{a}}{aH^3}, \quad s = \frac{(r-1)}{3(q-1/2)}, \tag{1}$$

where q is the deceleration parameter. From Eqs. (1), we see that the statefinder parameters depend only on the scale factor a and therefore constitute a geometrical diagnosis. The statefinder is a geometric diagnosis and makes it possible to distinguish the properties of dark energy in a model independently. The statefinder is dimensionless and is constructed from the scale factor of the universe and its time derivatives only. The parameter r is seen as a future step among the geometric cosmological parameters after the Hubble H parameter and the deceleration parameter q, s is a linear combination of q and r chosen so that it does not depend on the density of dark energy. The statefinder pair r, s is algebraically linked to the state equation of dark energy. The statefinder pair can be determined with great precision from an SNAP-type experiment. In the $r-s$ plane, the different types of dark energy models have different evolution paths, which makes it possible to identify each dark energy model with a trajectory. For example, for the quintessence and ghost models, trajectory is between the points $r < 1$ and $s > 0$, for the Chaplygin gas models, the trajectories are in the regions $s < 0$, $r > 1$. While quintessence models and Chaplygin gas models have typical trajectories similar to parabolic arcs (ascending and descending), for the phantom model, trajectories are different.[18] For the LCDM model (or ΛCDM), consisting of vacuum energy and dark or black masses, the statefinder parameters correspond to the fixed torque $\{r = 1, s = 0\}$.

Recently, Kanfon *et al.*[19] introduced a model of quintessence: the exponential harmonic field. The harmonic exponential field is important in cosmology since it

offers an alternative with regard to the dark matter models. The harmonic exponential field is part of these noncanonical field models proposed to express dark energy. This model could explain observational data since we have studied the phenomenon of inflation and the values observed are in agreement with those observed. In 2018 and 2019, the exponential harmonic field was used to study, respectively, the transition of the universe from the deceleration phase to the recent accelerated expansion phase[20] and the inflationary phenomenon through the parametrization of the state equation.[21] So far, the trajectory of the statefinder parameters is not studied with the exponential field. That justifies the goal of the present work in which. We will make the statefinder diagnosis of the exponential harmonic field model in order to see if it is distinguishable from the others. To achieve this, we use a method used by Ref. 22 in cosmological models within modified gravity theories, with extended nonminimal derivative couplings. This method has never been used to study statefinder parameters. We use it in this paper to study the statefinder parameters and the behavior of these parameters in the r, s plane with the harmonic exponential field.

The paper is organized as follows. First, we describe the model of the exponential field to be used, in second step, we adopt the method used by Ref. 22 to determine the statefinder parameters of the exponential harmonic field and finally we present the obtained results.

2. Exponential Harmonic Field

2.1. *Model*

We consider the action where

$$F(\phi, e(\phi)) = \exp\left(\frac{\lambda\dot{\phi}^2}{2}\right) - 1 - V(\phi)\,, \tag{2}$$

where $e(\phi) = \lambda\dot{\phi}^2/2$, λ is the parameter of normalization; $V(\phi)$ is the potential. Additionally, variation of the action with respect to ϕ provides the Klein Gordon equation:

$$\ddot{\phi}(1 + \lambda\dot{\phi}^2) + 3H\dot{\phi} + \frac{V'(\phi)}{\lambda}e^{\left(-\frac{\lambda}{2}\dot{\phi}^2\right)} = 0\,. \tag{3}$$

In the following, we focus on a spatially flat Friedmann–Robertson–Walker (FRW) background metric of the form

$$ds^2 = dt^2 + a^2(t)\delta^{ij}\,dx_i\,dx_j\,, \tag{4}$$

where t is the cosmic time, x^i the comoving spatial coordinates and $a(t)$ is the scale factor.

One have obtained the Friedmann equations as follows:

$$3H^2 = k^2\left[\frac{1}{2}e^{\left(\frac{\lambda}{2}\dot{\phi}^2\right)}\left(-1 + \lambda\dot{\phi}^2\right) + \frac{1}{2} + V(\phi) + T_{00}^m\right] \tag{5}$$

and

$$2\dot{H} + 3H^2 = k^2\left[-\frac{1}{2}e^{\left(\frac{\lambda}{2}\dot{\phi}^2\right)} + \frac{1}{2} + V(\phi) + T_{11}^m\right], \tag{6}$$

where $k^2 = 8\pi G$.

The state of diagnostic is one of the methods used to describe dark energy models. This is a method characterized by a geometric pair r, s that depends on the deceleration parameter q and the Hubble parameter H. Using both the second and third derivatives of the scale factor a, the statefinder r and s are defined by

$$r = \frac{\dddot{a}}{aH}, \quad s = \frac{r-1}{3\left(q-\frac{1}{2}\right)} \tag{7}$$

with $q \neq \frac{1}{2}$. This method makes it possible to distinguish the different models of dark energy. In the r, s diagram, one generally obtains a divergent behavior of the dark energy model. For example, in a flat universe FRW, one obtains in the diagram r, s a pair of fixed points $0, 1$ for the model $\wedge$CDM, on the other hand one identifies the fixed point $1, 1$ with the model SCDM in the same diagram. With this analysis, we can distinguish the models of dark energy like the model of quintessence, the model of the Chaplygin gas, the braneworld model and others.

We study here the statefinder parameters diagnostics as functions of the redshift z in the model of the exponential harmonic field by adopting the method used in Ref. 22. Let us start by writing Eq. (7) according to the parameter of Hubble H. By referring to t we have

$$r = 1 + 3\frac{\dot{H}}{H^2} + \frac{\ddot{H}}{H^3}, \quad s = \frac{r-1}{3\left(q-\frac{1}{2}\right)}, \tag{8}$$

where the deceleration parameter q is defined as follows:

$$q = -1 - \frac{\dot{H}}{H^2}. \tag{9}$$

2.2. *Method*

In this section, we express the parameters of the statefinder diagnostic and the deceleration parameter according to the redshift z. We use the Friedmann equations from the field equations (5) and (6). We can use the redshift z, defined as[22]

$$1 + z = \frac{a_0}{a}. \tag{10}$$

From now we have posed $a_0 = 1$. Thus, time derivatives can be expressed as[22]

$$\frac{d}{dt} = -H(z)(1+z)\frac{d}{dz}. \tag{11}$$

By combining (5) and (6), and making use of (3), one obtains the following system

$$\begin{cases} 4\dot{H} + 12H^2 = e^{\left(-\frac{\lambda}{2}\dot{\phi}^2\right)}(-2 + \lambda\dot{\phi}^2) + 2 + 4V(\phi) + 2\rho_m + 2p_m, \\ \ddot{\phi}(1 + \lambda\dot{\phi}^2) + 3H\dot{\phi} + \dfrac{V'(\phi)}{\lambda}e^{\left(-\frac{\lambda}{2}\dot{\phi}^2\right)}. \end{cases} \tag{12}$$

Let us introduce some dimensionless way parameters

$$\tau = H_0 t\,, \quad H = H_0 h\,, \quad \phi = H_0 \Phi\,,$$
$$\lambda = \frac{\mu}{H_0^2}\,, \quad V(\phi) = 3H_0 V(\Phi)\,, \tag{13}$$
$$\rho_m = 3H_0 r\,, \quad P_m = 3H_0 P\,.$$

From (10) and (13) we have

$$\dot{\phi} = H_0 \frac{d\Phi}{d\tau}\,, \quad \ddot{\phi} = H_0^2 \frac{d^2\Phi}{d\tau^2}\,, \quad \dot{H} = H_0^2 \frac{dh}{d\tau} \tag{14}$$

for reasons of simplification, and normalized H_0 to unity. Using Eqs. (14), the system (12) becomes

$$\begin{cases} \dfrac{d\Phi}{d\tau} = B\,, \\ \dfrac{dh}{d\tau} = -3h^2 + \dfrac{1}{4} e^{\left(\frac{\mu}{2}B^2\right)}\left(-2 + \mu B^2\right) + \dfrac{1}{2} + \dfrac{V(\Phi)}{2} + \dfrac{1}{2} r + \dfrac{1}{2} p\,, \\ \dfrac{dB}{d\tau} = -\dfrac{3hB}{1+\mu B^2} + \dfrac{V'(\Phi)}{\mu(1+\mu B^2)} e^{-\left(\frac{\mu}{2}B^2\right)}\,. \end{cases}$$

The dimensionless time-redshift relation (11) becomes

$$\frac{d}{d\tau} = -h(z)(1+z)\frac{d}{dz}\,,$$

$$\begin{cases} \dfrac{d\Phi}{dz} = -\dfrac{B}{h(1+h)}\,, \\ \dfrac{dh}{dz} = \dfrac{3h}{1+z} - \dfrac{e^{\left(\frac{\mu}{2}B^2\right)}\left(-2+\mu B^2\right)}{4(1+z)h} - \dfrac{1}{2(1+z)h} - \dfrac{V(\Phi)}{2(1+z)h} - \dfrac{r+P}{2(1+z)h}\,, \\ \dfrac{dB}{dz} = -\dfrac{3hB}{\left(1+\mu B^2\right)(1+z)} + \dfrac{V'(\Phi)}{\mu\left(1+\mu B^2\right)(1+z)} e^{-\left(\frac{\mu}{2}B^2\right)}\,. \end{cases} \tag{15}$$

Now we consider the time evolution of a dust matter fluid, namely, we assume $P = 0$, and hence the redshift dependence of the auxiliary matter energy density is given by $r = (1+z)^3$, so, from (15) we obtain

$$\begin{cases} \dfrac{d\Phi}{dz} = -\dfrac{B}{h(1+h)}\,, \\ \dfrac{dh}{dz} = \dfrac{3h}{1+z} - \dfrac{e^{\left(\frac{\mu}{2}B^2\right)}\left(-2+\mu B^2\right)}{4(1+z)h} - \dfrac{1}{2(1+z)h} - \dfrac{V(\Phi)}{2(1+z)h} - \dfrac{(1+z)^2}{2h}\,, \\ \dfrac{dB}{dz} = -\dfrac{3B}{(1+\mu B^2)(1+z)} + \dfrac{V'(\Phi)}{\mu(1+\mu B^2)(1+z)} e^{-\left(\frac{\mu}{2}B^2\right)}\,. \end{cases}$$

The statefinder parameters (8) become

$$\begin{aligned} r &= 1 + \frac{(1+z)^2}{h}\frac{d^2h}{dz^2} + \frac{(1+z)^2}{h^2}\left(\frac{dh}{dz}\right)^2 - 2\frac{(1+z)}{h}\frac{dh}{dz}\,, \\ s &= \frac{\frac{(1+z)^2}{h}\frac{d^2h}{dz^2} + \frac{(1+z)^2}{h^2}\left(\frac{dh}{dz}\right)^2 - 2\frac{(1+z)}{h}\frac{dh}{dz}}{3\left(q-\frac{1}{2}\right)} \end{aligned} \tag{16}$$

with

$$\begin{aligned} \frac{d^2h}{dz^2} &= -\frac{1}{h}\left(\frac{dh}{dz}\right)^2 + 5\left(\frac{1}{1+z}\right)\frac{dh}{dz} \\ &\quad + \frac{\mu^2B^2}{4h(1+z)}\frac{dB}{dz}e^{\frac{\mu}{2}B^2} + \frac{3V'B}{2h^2(1+z)^2} - \frac{9r_0}{2h(1+z)}\,. \end{aligned} \tag{17}$$

2.3. *Results*

In the following curves, we take $\mu = 0.1$, $\alpha = -1.5$ and $\beta = 0.5$. By changing alpha and beta, and by taking values close to those above, the shape of the curves does not change fundamentally.

2.3.1. *Exponential potential*: $V(\Phi) = V_0 e^{-\alpha\Phi^2}$

Using the exponential potential,[24] Eq. (16) yields

$$\begin{cases} \dfrac{d\Phi}{dz} = -\dfrac{B}{h(1+h)}\,, \\ \dfrac{dh}{dz} = \dfrac{3h}{1+z} - \dfrac{e^{\left(\frac{\mu}{2}B^2\right)}\left(-2+\mu B^2\right)}{4(1+z)h} - \dfrac{1}{2(1+z)h} - \dfrac{V_0e^{-\alpha\Phi^2}}{2(1+z)h} - \dfrac{(1+z)^2}{2h}\,, \\ \dfrac{dB}{dz} = -\dfrac{3hB}{(1+\mu B^2)(1+z)} - \dfrac{2\alpha V_0\Phi e^{-\alpha\Phi^2}}{\mu(1+\mu B^2)(1+z)}e^{-\left(\frac{\mu}{2}B^2\right)}\,. \end{cases}$$

2.3.2. *Power-law potential*

Using power-law potential of type $V(\phi) = V_0\phi^\beta$, Ref. 23, Eq. (16) gives

$$\begin{cases} \dfrac{d\Phi}{dz} = -\dfrac{B}{h(1+h)}\,, \\ \dfrac{dh}{dz} = \dfrac{3h}{1+z} - \dfrac{e^{\left(\frac{\mu}{2}B^2\right)}\left(-2+\mu B^2\right)}{4(1+z)h} - \dfrac{1}{2(1+z)h} + \dfrac{V_0\Phi^2}{2(1+z)h} - \dfrac{(1+z)^2}{2h}\,, \\ \dfrac{dB}{dz} = -\dfrac{3hB}{\left(1+\mu B^2\right)(1+z)} + \dfrac{\beta V_0\Phi^{\beta-1}}{\mu\left(1+\mu B^2\right)(1+z)}e^{-\left(\frac{\mu}{2}B^2\right)}\,. \end{cases}$$

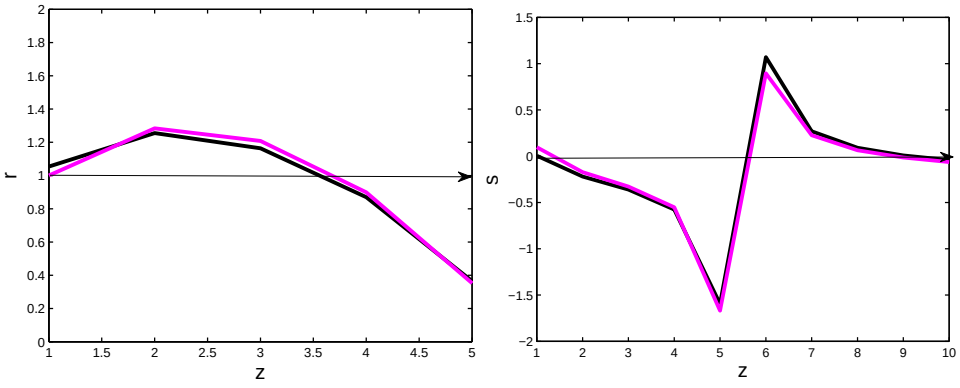

(a) (b)

Fig. 1. (Color online) (a) Evolution of the statefinder pair r, z for the exponential harmonic field with exponential potential. (b) Evolution of the statefinder pair s, z for the exponential harmonic field for the exponential potential. ($\phi_0 = -0.1$, $h_0 = 0.01$, $B_0 = 0.40$) for black curves and ($\phi_0 = -0.2$, $h_0 = 0.01$, $B_0 = 0.30$) for pink curves.

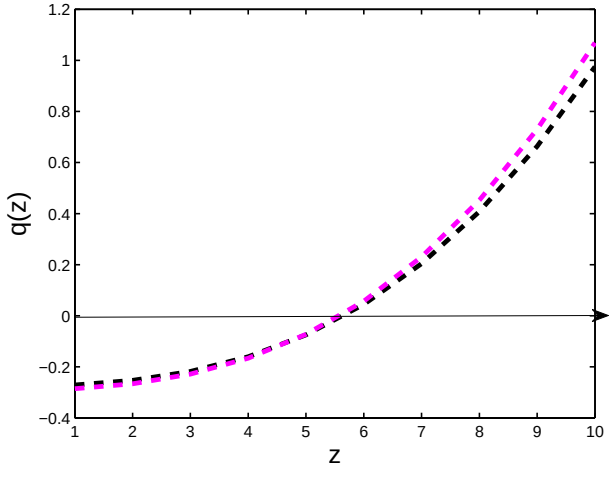

Fig. 2. (Color online) The behavior of the deceleration parameter q over z for the exponential harmonic field with exponential potential. ($\phi_0 = -0.1$, $h_0 = 0.01$, $B_0 = 0.40$) for black curve and ($\phi_0 = -0.2$, $h_0 = 0.01$, $B_0 = 0.30$) for pink curve.

3. Analysis

Figures 3(b) and 6(b) show the behavior of r as a function of q. We note an attraction of the SCDM model ($r = 1$, $s = 0.5$) to the LCDM model ($r = 1$, $S = -1$). Figures 3(a) and 6(a) represent the temporal evolution of the pair (r, s). Note that the curves are in the form of ascending and descending parabola in the region $r < 1$ and $s > 0$. We also note a convergence towards the LCDM model ($r = 1$, $s = 0$). From what precedes, one can affirm that it is about a quintessence model. In Figs. 1

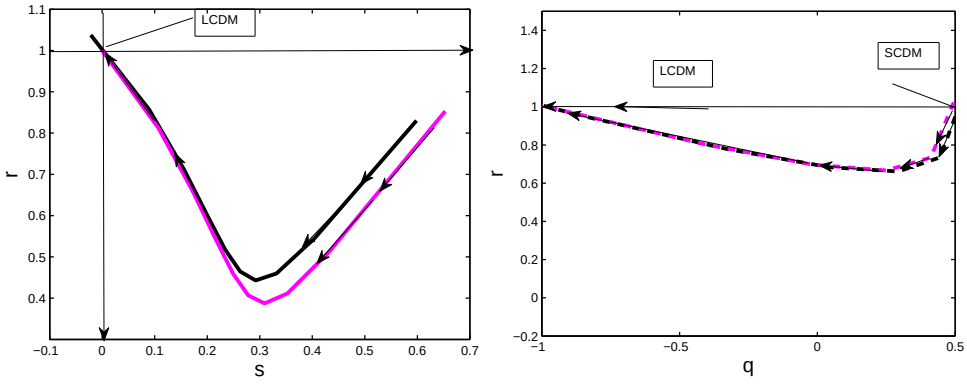

(a) (b)

Fig. 3. (Color online) (a) Evolution of the statefinder parameter r over s for exponential harmonic field model with exponential potential. (b) Evolution of r over q for the exponential harmonic field with exponential potential. ($\phi_0 = -0.1$, $h_0 = 0.01$, $B_0 = 0.40$) for black curves and ($\phi_0 = -0.2$, $h_0 = 0.01$, $B_0 = 0.30$) for pink curves.

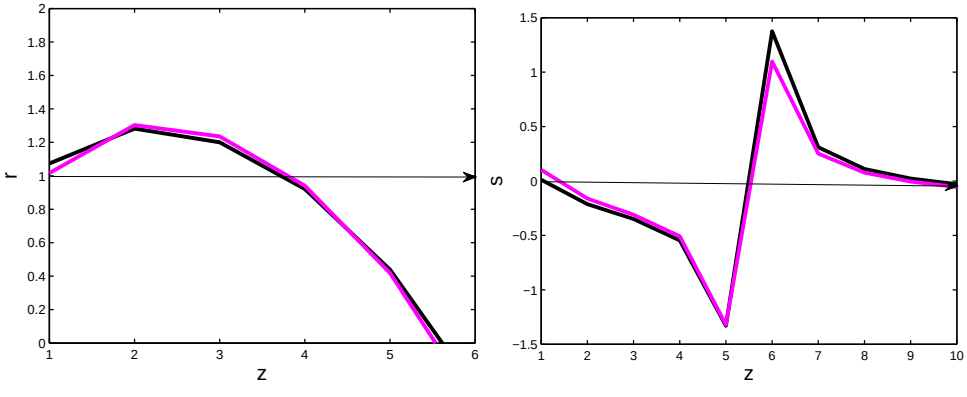

(a) (b)

Fig. 4. (Color online) (a) Evolution of the statefinder pair r, z for the exponential harmonic field with power-law potential. (b) Evolution of the statefinder pair s, z for the exponential harmonic field for power-law potential. ($\phi_0 = -0.1$, $h_0 = 0.01$, $B_0 = 0.40$) for black curves and ($\phi_0 = -0.2$, $h_0 = 0.01$, $B_0 = 0.30$) for pink curves.

and 4, the statefinder parameters are numerically studied as functions of the redshift ($r - z$, $s - z$). These analysis show a real transition between the deceleration phase and the acceleration phase of the universe. In Figs. 2 and 5, one can note that curves $q(z)$ close at $z = 1$ because this value constitutes one of the statefinder characteristics of the CDM model, which means that studied model is getting closer to the latter. The exponential potentials and power-law potentials have minimal effects on the behavior of the curves. This is why the curves are almost similar for the two potentials.

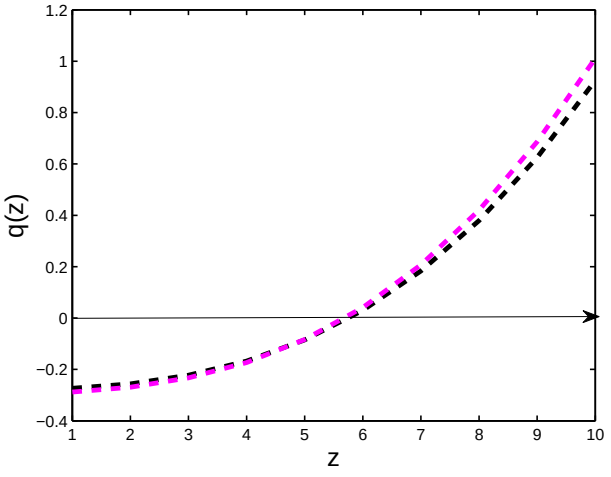

Fig. 5. (Color online) Behavior of $q(z)$ for the exponential harmonic field with power-law potential, ($\phi_0 = -0.1$, $h_0 = 0.01$, $B_0 = 0.40$) for black curve and ($\phi_0 = -0.2$, $h_0 = 0.01$, $B_0 = 0.30$) for pink curve.

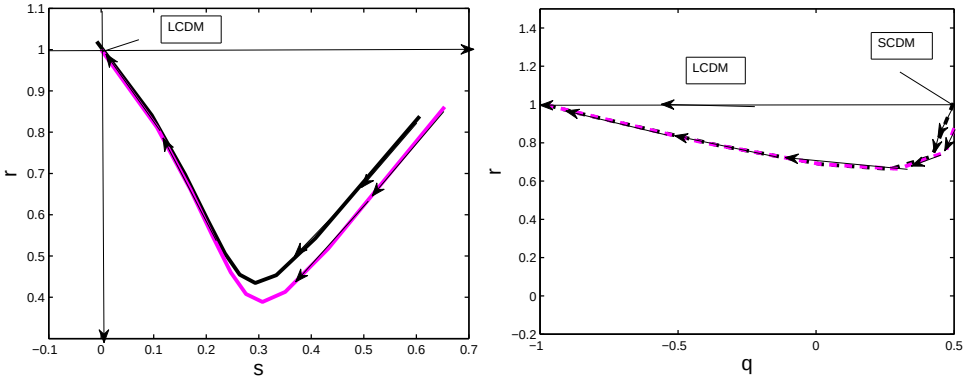

(a) (b)

Fig. 6. (Color online) (a) Behavior of the statefinder parameter r over s for exponential harmonic field model with the power-law potential. (b) Behavior of r over q for the exponential harmonic field with the power-law potential. ($\phi_0 = -0.1$, $h_0 = 0.01$, $B_0 = 0.40$) for black curves and ($\phi_0 = -0.2$, $h_0 = 0.01$, $B_0 = 0.30$) for pink curves.

4. Conclusion

In this paper, we studied the behavior of the exponential harmonic field in a FLRW universe based on the statefinder parameters. In a first step, we determined the statefinder parameters according to the redshift by the method developed by Harko *et al.*[22] We then performed a numerical analysis of the pairs (r, s), (r, z), (s, z), (r, q), (q, z). The curves obtained in particular (s, z) and (r, z) cross the LCDM model, thus showing the transition between the accelerated phase and the decelerated

phase of the universe. This thesis is confirmed by the curves (q, z). The shape of the curves (r, q) shows an attracting effect of the SCDM model ($r = 1$, $q = 0.5$) toward the LCDM one ($r = 1$, $q = -1$). We can confirm that this method presents an effective way of distinguishing different models of dark energy.

References

1. A. G. Riess *et al.*, *Astron. J.* **116**, 1009 (1998).
2. S. Perlmutter *et al.*, *Astrophys. J.* **517**, 565 (1999).
3. J. L. Tonry *et al.*, *Astrophys. J.* **594**, 1 (2003).
4. B. J. Barris *et al.*, *Astrophys. J.* **602**, 571 (2004).
5. A. G. Riess *et al.*, *Astrophys. J.* **607**, 665 (2004).
6. M. Hu and X. Meng, *Phys. Lett. B* **635**, 4 (2006).
7. D. N. Spergel *et al.*, *Astrophys. J. Suppl.* **148**, 175 (2003).
8. B. Chang, H. Liu, L. Xu, C. Zhang and Y. Ping, *J. Cosmol. Astropart. Phys.* **2007**, 016 (2007).
9. C. Wetterich, *Nucl. Phys. B* **302**, 668 (1988).
10. B. Ratra and P. E. J. Peebles, *Phys. Rev. D* **37**, 3406 (1988).
11. R. R. Caldwell, *Phys. Lett. B* **545**, 23 (2002).
12. P. Singh, M. Sami and N. Dadhich, *Phys. Rev. D* **68**, 023522 (2003).
13. K. Nozari and N. Rashidi, *Phys. Rev. D* **88**, 023519 (2013).
14. B. Feng, X. L. Wang and X. M. Zhang, *Phys. Lett. B* **607**, 35 (2005).
15. A. Kamenshchik, U. Moschella and V. Pasquier, *Phys. Lett. B* **511**, 26 (2001).
16. Z. Zhu, *Astron. Astrophys.* **421**, 423 (2004).
17. V. Sahni, T. D. Saini, A. A. Starobinsky and U. Alam, *JETP Lett.* **77**, 201 (2003), arXiv:astro-ph/0201498.
18. P. Wu and H. Yu, *Int. J. Mod. Phys. D* **14**, 11 (2005).
19. D. A. Kanfon, D. A. Fuzfa and D. Lambert, *J. Phys. A*: *Math. Gen.* **35**, 7629 (2002).
20. A. D. Kanfon and F. Mavoa, *J. Astrophys. Astron.* **39**, 62 (2018).
21. A. D. Kanfon and F. Mavoa, *J. Astrophys. Astron.* **40**, 2 (2019).
22. T. Harko, N. S. F. Lobo, N. E. Saridakis and M. Tsoukalass, *Phys. Rev. D* **95**, 044019 (2017).
23. V. Sahni, Exploring dark energy using the statefinder, arXiv:astro-ph/0211084v1.
24. W.-Z. Liu, *Int. J. Mod. Phys. D* **18**, 1 (2009).